

Effect of Long-term Thermal Aging on Microstructure and Mechanical Property Changes of Fe-15Cr Ferritic Alloys

Dongsheng CHEN¹, Akihiko KIMURA², Wentuo HAN², Wenyue TANG³

¹Graduate School of Energy Science, Kyoto University, Gokasho, Uji, Kyoto 611-0011, Japan

²Institute of Advanced Energy, Kyoto University, Gokasho, Uji, Kyoto 611-0011, Japan

³Beijing Huairou Vocational School, Beijing 100047, China

(Received: 13 September 2014 / Accepted: 19 January 2015)

The effects of long-term thermal aging on the mechanical and microstructural behaviors of Fe-15Cr ferritic alloys were investigated and the mechanism of strengthening was proposed with relevant to the size of Cr-rich α' precipitates. Arc melting was used to produce Fe-15Cr alloys named Fe-Cr, Fe-Cr-C and Fe-Cr-Xs, where Xs referred to Si, Mn and Ni to investigate the effect of G-phase on age-hardening. Detailed microstructural characterization before and after aging at 475°C up to 10,000 h was conducted to understand the impact of alloying elements on aging embrittlement; microstructural information before and after tensile deformation, including grain morphology, dislocation and precipitates, was obtained using SEM, TEM. Ductility loss of Fe-Cr-Xs alloy was found different with other alloys; EBSD was used to elucidate the difference in the microstructure. Thermal aging results in two stages of changes in the strength: age hardening with increasing aging period then followed by over-aging. The critical size of α' precipitates for the appearance of over-aging is around 8 nm in diameter.

Keywords: high chromium ferritic alloys, phase decomposition, chromium rich precipitates, mechanical properties, age hardening, over aging.

1. Introduction

High-Cr ferritic steels are of technology interest for advanced fusion blankets as well as nuclear power plants [1-3]. There is, however, a trade-off issue of corrosion resistant and aging embrittlement, which is attributed to the phase decomposition to Fe rich α phase and Cr rich α' phase. Binary Fe-Cr alloys exhibit α/α' phase decomposition if the Cr content exceeds ~12 wt. %, in the region of temperatures potentially important for technological applications (300~550 °C) [4-7].

Until now, there are several reports on the impact of α/α' phase decomposition on mechanical property changes in Fe-Cr alloys [8-13]. Cr-rich phases are a bit oversized coherent body-centered cubic (bcc) particles, with higher shear modulus than Fe-rich matrix [8]. Precipitates formed by α/α' phase decomposition harden the material because they obstruct the motion of dislocations. A few experiments done for neutron irradiated Fe-Cr alloys suggest that the substantial contribution to the irradiation hardening comes from the difficulty for edge dislocations shearing Cr-rich precipitates [12]. The Cr rich α' precipitation leads to a progressive hardening and deterioration of fracture toughness.

Effect of alloying elements on aging embrittlement of high Cr ferritic alloys has been studied [14-16].

According to Mueller [14], who studied the effect of varying carbon contents on the impact energy of Fe-17wt. % Cr alloys, there is a small increase in DBTT as the carbon content increases. Courtnall et al. [15] found that embrittlement was enhanced by the addition of substitutional elements, such as Ti and Nb. As for the effect of alloy elements in the ferritic steels, it was reported that the G-phases were formed after long term aging over 8,000 h, and age hardening was enhanced [16]. However, the influence of alloying elements and α/α' phase decomposition on aging hardening behaviors of Fe-Cr alloys is still not thoroughly understood.

In this work, long-term thermal aging effect on the mechanical and microstructural behaviors Fe-15Cr alloys was investigated up to the aging period of 10,000 h, using transmission electron microscopy (TEM), scanning electron microscopy (SEM) and tensile tests. Effect of alloying elements as well as the size of α' precipitates on age-hardening was focused.

2. Experimental

The materials used in this study were Fe-15Cr alloys, named Fe-Cr, Fe-Cr-C and Fe-Cr-Xs, with keeping Cr content around 15 wt. %. The chemical compositions are shown in Table 1. Fe-Cr-C was added with 0.02 wt. % carbon. Fe-Cr-Xs was added with Mn, Si and Ni to investigate the effect of G-phase formation on

Author's e-mail: ds-chen@iae.kyoto-u.ac.jp

age-hardening.

Table 1 Chemical compositions of the alloys (wt. %).

Materials	Cr	C	Mn	Si	Ni	Fe
Fe-Cr	14.55	0.001	-	-	-	Bal.
Fe-Cr-C	14.83	0.022	-	-	-	Bal.
Fe-Cr-Xs	14.96	0.002	0.83	0.51	0.49	Bal.

The model alloys were fabricated by arc melting method in argon atmosphere. The alloy button ingots ($\phi 30\text{mm} \times 5\text{mm}$ thickness) were first homogenized at 1100 °C for 72 h followed by furnace cooling, and then cold rolled by 80% at room temperature. All the specimens were punched out from the alloy sheet with 0.3 mm thick, and finally annealed at 900 °C for 2h followed by iced water quenching. Some of specimens were sealed in quartz tube in high vacuum conditions (10^{-4} Pa) and isothermally aged at 475 °C for up to 10,000 h.

Tensile tests were carried out at room temperature by using an INTESCO tensile testing machine with a crosshead velocity of 0.2 mm/min. Tensile test specimens, which had a dimension of 4mm width \times 16mm length \times 0.25mm thickness were fabricated parallel to the rolling direction. At least three measurements were made and averaged. The grain morphology and ruptured surfaces of tensile specimens were examined using a Zeiss Ultra 55 FESEM, equipped with an electron backscatter diffraction (EBSD) system. Disk-type specimens of 3mm diameter were punched out from the sheets and mechanically thinned to ~ 100 μm . Specimens for TEM observation were prepared using a twin jet electro-polishing method with a solution composed of 10 vol. % perchloric acid and 90 vol. % acetic acid at room temperature. TEM observation has been performed using a JEOL 2100 operating at 200 kV. The thickness of thin foils was measured using convergent beam electron diffraction (CBED) technique.

3. Results and discussion

3.1 Tensile properties

Thermal aging at 475°C causes a significant increase in strength accompanied with corresponding decrease in total elongation. Fig. 1 shows the change in yield stress (YS), ultimate tensile stress (UTS) and total elongation as a function of aging time. As aging time increases to 5,000 h, yield stresses increase after an incubation period for all the materials. While after aging for 10,000 h, the tensile stresses decrease slightly as compared to the peak values.

Fig. 2 provides the relations between the change in yield stress, $\Delta\sigma_y$, and the change in total elongation, $\Delta\epsilon$, of each alloy during aging for different time. There is a linearity between $\Delta\sigma_y$ and $-\Delta\epsilon$ for all the alloys. The slopes of the plots, $\Delta\sigma_y/-\Delta\epsilon$ of each alloy are classified into two groups, one is Fe-Cr and Fe-Cr-C and the other

is Fe-Cr-Xs, which is represented in a gray area in Fig. 2. It is considered that the ductility loss of Fe-Cr-Xs needs a larger age-hardening than that of Fe-Cr and Fe-Cr-C.

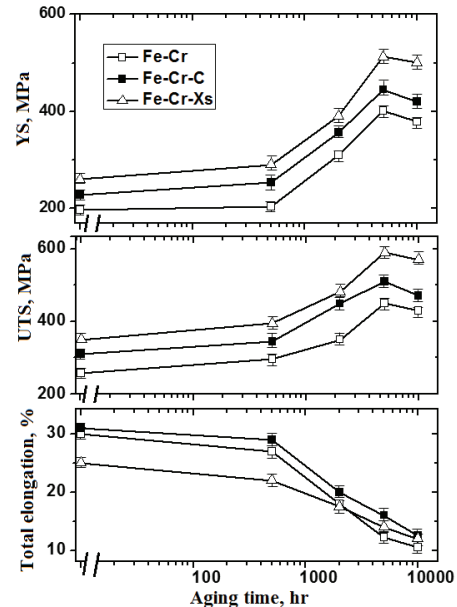


Fig. 1 Evolution of yield stress, ultimate tensile stress and elongation during aging at 475°C.

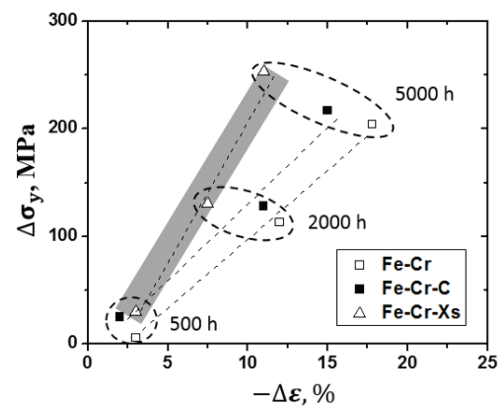


Fig. 2 Linear relations between the change in yield stress, $\Delta\sigma_y$, and the change in elongation, $-\Delta\epsilon$, of each alloy.

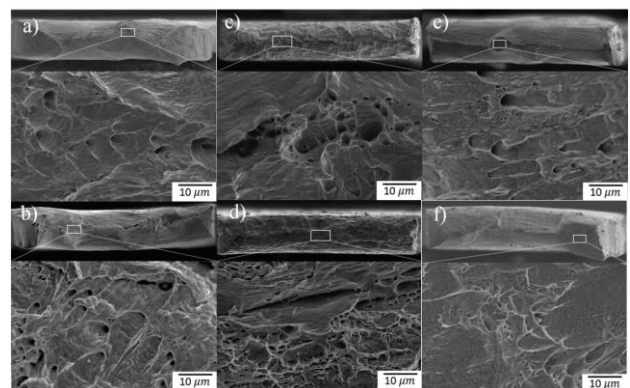


Fig. 3 Ruptured surfaces of the model alloys: a) Fe-Cr, unaged; b) Fe-Cr, aged for 10,000 h; c) Fe-Cr-C, unaged; d) Fe-Cr-C, aged for 10,000 h; e) Fe-Cr-Xs, unaged; f) Fe-Cr-Xs, aged for 10,000 h.

3.2 Ruptured surfaces observation

Fig. 3 shows the ruptured surfaces of the model alloys deformed at room temperature before and after aging at 475 °C for 10,000 h. Before and after aging, all the alloys rupture in a ductile manner, indicating that the DBTTs of all the specimens are below room temperature even after aging up to 10,000 h.

3.3 Microstructures

TEM bright field images of the model alloys are shown in Fig. 4. Before aging, as presented in Fig. 4(a), almost no precipitates exist in Fe-Cr alloy as well as other alloys except for a small amount of grain boundary precipitates. Some lath shaped structures are observed in the ferrite matrix of Fe-Cr-Xs alloy, as shown in Fig. 4(b). A large number of dislocations can be observed in these structures or along their interface with ferrite.

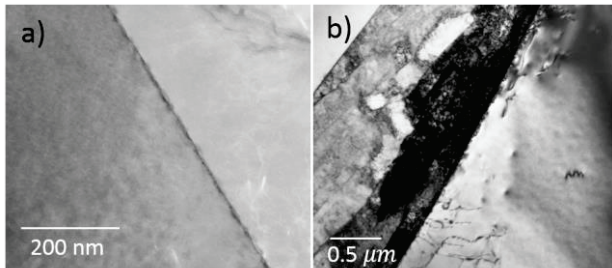


Fig. 4 TEM bright field images of a) Fe-Cr alloy, unaged, b) Fe-Cr-Xs alloy, unaged.

After tensile testing, the grain morphology and ruptured region of Fe-Cr-Xs alloy aged for 5000 h were examined by EBSD, as presented in Fig. 5. The EBSD maps were acquired from the side surface paralleling to RD&TD plane by removing 0.1mm thickness. The orientation of tensile specimens is defined as: RD (rolling direction), TD (transverse direction) and ND (normal direction). A transgranular fracture was found in Fe-Cr-Xs alloy, as shown in the marked area in Fig. 5(a). Some phases in ferrite matrix are characterized as tempered martensite, as presented in Fig. 5(b).

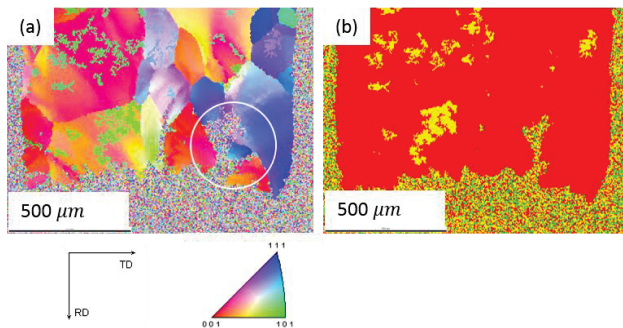


Fig. 5 Fe-Cr-Xs alloy after aged for 5000 h: (a) grain morphology of the ruptured region; (b) phase characterization, ferrite (red color) and martensite (yellow).

3.4 Precipitates

The addition of carbon leads to the precipitation of Cr rich $M_{23}C_6$ and Fe_2C carbides on or nearby grain boundaries, as presented in Fig. 6(a). In Fe-Cr-Xs alloy, there are also some Cr rich $M_{23}C_6$ carbides precipitations. TEM EDS X-ray analysis shows that the Cr content in martensite is lower than 12 wt. %. This result can explain why there is no phase decomposition structure observed in martensite, as shown in Fig. 6(b).

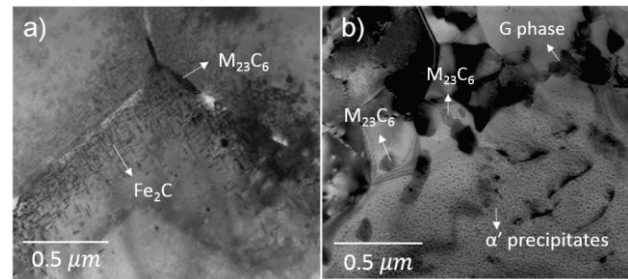


Fig. 6 TEM bright field images of a) Fe-Cr-C alloy, aged for 500 h, b) Fe-Cr-Xs alloy, aged for 5000 h.

The loss of elongation during aging is mainly due to α/α' phase decomposition. Thus, the reason why Fe-Cr-Xs alloy shows smaller ductility loss than other alloys can be attributed to the formation of martensitic phase, in which phase decomposition is not easy to occur. However, along the interface of ferrite and martensitic phase, there are some amount of carbides and few Si-Cr-Mn enriched G phases, which can increase the embrittlement of the material. It is considered that the transgranular fracture characterized by EBSD is due to the formation of Cr rich α' precipitates as well as carbides and G phases in Fe-Cr-Xs alloy.

3.5 Critical size of α' precipitates for over-aging

Fig. 7 shows α/α' phase decomposition of Fe-Cr alloy observed by TEM. Cr rich α' precipitates shows coherent contrast because of the similar lattice parameter of Fe and Cr. Our previous research [17] showed that the main reason of age-hardening is due to the formation of α' precipitates.

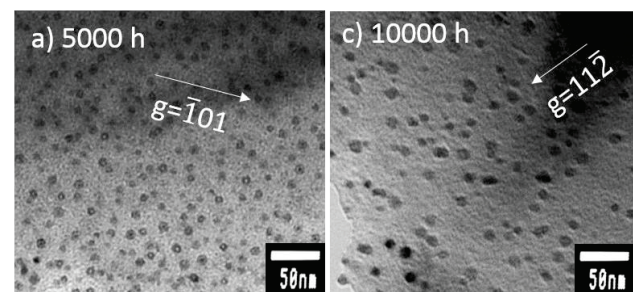


Fig. 7 TEM bright field images of a) Fe-Cr, aged for 5000 h, b) Fe-Cr, aged for 10,000 h.

With increasing aging time, the average size of α' precipitates increase while the number density decreases. As aging time increases from 500 h to 5000 h, α' precipitates become larger, with averaged diameter increasing from 2 nm to about 8 nm. When aging time reaches up to 10,000 h, averaged diameter of α' precipitates increases to about 11 nm with number density decreasing from $2.1 \times 10^{22} \text{ m}^{-3}$ (5000 h) to $1.2 \times 10^{22} \text{ m}^{-3}$. The present results indicate that the strength decreases slightly, although α' precipitates continue coarsening.

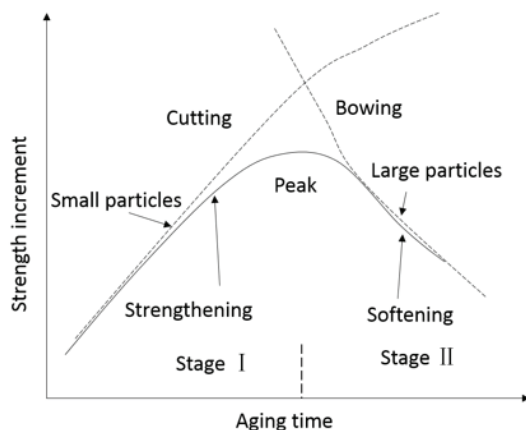


Fig. 8 Age-hardening curve and sketch diagram for precipitation hardening mechanism.

When aging time reaches at 10,000 h, thermal aging undergoes an over-aging, which leads to a decreasing hardness. Fig. 8 shows a sketch map of precipitation strengthening curve of Fe-15Cr alloys. We may define the critical particle size as d_c , then:

- (1) when $d < d_c$, coherency strengthening increases with increasing particle size;
- (2) when $d > d_c$, coherency strengthening decreases with increasing particle size.

Such a relationship between strengthening effect and particle size gives a maximum strengthening at a critical particle size d_c . According to current data, the critical d_c for Fe-15Cr alloy is about 8 nm.

It is considered that dislocation looping can take place whenever the precipitates is too big/strong for dislocation to cut through, regardless of the coherency nature of the interface between the precipitate and matrix.

Another issue beyond 10,000 h is the continuous effect of G-phase precipitation. Since Fig. 1 indicates that the reduction of strength after 5,000 h is a little bit smaller in Fe-Cr-Xs alloy than the others, it can be expected that G-phase precipitation starts to contribute to the hardening. The alloys without Ni, Mn and Si additions only show so-called Ostwald ripening of Cr rich phases. Further longer aging period is necessary to confirm the effect of G-phase precipitation on the age-hardening.

4. Conclusions

The effects of long-term isothermal aging (up to 10,000 h, 475°C) on microstructure and mechanical property changes in Fe-15Cr alloys have been investigated. The main results are summarized as follows:

- (1) Thermal aging causes a remarkable increase in strength with corresponding decrease in elongation. The lower ductility loss in Fe-Cr-Xs alloy is related to the formation of few tempered martensitic phases, in which phase decomposition is not observed.
- (2) Even after 10,000 h aging, all the materials rupture in a ductile manner.
- (3) The addition of alloying elements leads to the formations of carbides and G phases. Cr-rich α' precipitates as well as carbides and G phase are considered to be the source of appearance of age hardening.
- (4) Age-hardening shows two stages, showing a peak in the strength with increasing aging period, which is associated with the size of Cr-rich α' precipitates. The critical size for α' precipitates is around 8 nm.
- (5) Further aging is necessary to confirm the effect of alloying additions.

Acknowledgments

The authors would like to thank Dr. Chonghong Zhang and Dr. Sosuke Kondo for support with the TEM observation, and Mr. Yasunori Hayashi for support with EDS X-ray analysis. Financial support from China Scholarship Council and Institute of Advanced Energy, Kyoto University, is gratefully acknowledged.

References

- [1] A. Kimura *et al.*, *J Nucl Mater*, **417**, 176 (2011).
- [2] S. Ukai *et al.*, *J Nucl Sci Technol*, **39**, 872 (2002).
- [3] T. Yoshitake *et al.*, *J Nucl Mater*, **788**, 307 (2002).
- [4] R.M. Fisher *et al.*, *Trans AIME*, **197**, 690 (1953).
- [5] P. J. Grober, *Metall Trans*, **4**, 251(1973).
- [6] T.J. Nichol *et al.*, *Metall Trans A*, **11A**, 573(1980).
- [7] R.O. Williams, *Trans. TMS-AIME*, **212**, 497(1958).
- [8] J. Ribis, S. Lozano, *Mater Let*, **74**, 143 (2012).
- [9] G. Bonny *et al.*, *Phys Rev B*, **79**, 104 (2009).
- [10] K. Suganuma, H. Kayano, *J Nucl Mater*, **118**, 234 (1983).
- [11] O. Soriano-Vargas and E. O. Avila-Davila, *Mater Sci Eng A*, **527**, 2910 (2010).
- [12] D.A. Terentyev *et al.*, *Acta Mater*, **56**, 3229 (2008).
- [13] M. Bachhav *et al.*, *Scripta Mater*, **74**, 48 (2014).
- [14] E. Mueller, *Neue Heute*, **22(5)**, 273(1977).
- [15] M. Courtinall and F. B. Pickering, *Metal Science*, **10**, 273 (1976).
- [16] T. Hamaoka *et al.*, *Phil Mag*, **92**, 4354 (2012).
- [17] D. Chen, A. Kimura, W. Han, *J Nucl Mater*, **455**, 436 (2014).